Inorg. Chem. **2007**, *46*, 4989–4996

Sulfur K-Edge XAS and DFT Studies on Ni^{II} Complexes with Oxidized Thiolate Ligands: Implications for the Roles of Oxidized Thiolates in the Active Sites of Fe and Co Nitrile Hydratase

Abhishek Dey,[†] Stephen P. Jeffrey,[‡] Marcetta Darensbourg,[‡] Keith O. Hodgson,*[,†,§] Britt Hedman,*[,§] and Edward I. Solomon*[,†,§]

Department of Chemistry, Stanford University, Stanford, California 94305, Department of Chemistry, Texas A&M University, College Station, Texas 77843, and Stanford Synchrotron Radiation Laboratory, SLAC, Stanford University, Menlo Park, California 94025

Received February 7, 2007

S K-edge X-ray absorption spectroscopy data on a series of Ni^{II} complexes with thiolate (RS^-) and oxidized thiolate (RSO_2^-) ligands are used to quantify Ni–S bond covalency and its change upon ligand oxidation. Analyses of these results using geometry-optimized density functional theory (DFT) calculations suggest that the Ni–S σ bonds do not weaken on ligand oxidation. Molecular orbital analysis indicates that these oxidized thiolate ligands use filled high-lying S–O π^* orbitals for strong σ donation. However, the RSO_2^- ligands are poor π donors, as the orbital required for π interaction is used in the S–O σ-bond formation. The oxidation of the thiolate reduces the repulsion between electrons in the filled Ni t_2 orbital and the thiolate out-of-plane π-donor orbital leading to shorter Ni–S bond length relative to that of the thiolate donor. The insights obtained from these results are relevant to the active sites of Fe- and Co-type nitrile hydratases (Nhase) that also have oxidized thiolate ligands. DFT calculations on models of the active site indicate that whereas the oxidation of these thiolates has a major effect in the axial ligand-binding affinity of the Fe-type Nhase (where there is both σ and π donation from the S ligands), it has only a limited effect on the sixth-ligand-binding affinity of the Co-type Nhases (where there is only σ donation). These oxidized residues may also play a role in substrate binding and proton shuttling at the active site.

Introduction

Cysteine-based oxidized thiolate ligands (e.g., $CysSO_2^-$ and $CysSO^-$) in contiguous cysteine-serine-cysteine ligation have been found in nature in the active sites of Fe^{III}- and Co^{III}-dependent nitrile hydratases (Nhase).[1,2] These enzymes are key components in bioremediation of common plant metabolism byproducts.[3] The oxidation of these thiolates results from a post-translational modification upon exposure to dioxygen.[4] As the unoxidized active site of Fe-type Nhase is inactive, it is surmised that these oxidized thiolate ligands are key to reactivity.[5]

The role of the oxidized thiolate ligands in the active site of Nhase has received a great deal of attention, particularly for the Fe enzyme. Several model complexes have been synthesized that mimic the first coordination sphere of these enzymes including the S-coordinated, S-oxygenated ligands.[6–9] In general, these models lack the highly conserved H-bonding interactions from the protonated arginine residues to the negatively charged oxygen atoms of the RSO_x units (one to each unit) present at the active site.[10] Mutation of these

* To whom correspondence should be addressed. E-mail: Edward.Solomon@stanford.edu.
[†] Department of Chemistry, Stanford University.
[‡] Department of Chemistry, Texas A&M University.
[§] Stanford Synchrotron Radiation Laboratory, SLAC, Stanford University.

(1) Nagashima, S. N. M.; Dohmae, N.; Tsujimura, M.; Takio, K.; Odaka, M.; Yohda, M.; Kamiya, N.; Endo, I. *Nat. Struct. Biol.* **1998**, *5*, 347−351.
(2) Miyanaga, A.; Fushinobu, S.; Ito, K.; Wakagi, T. *Biochem. Biophys. Res. Commun.* **2001**, *288*, 1169−1174.
(3) Endo, I.; Nojiri, M.; Tsujimura, M.; Nakasako, M.; Nagashima, S.; Yohda, M.; Odaka, M. *J. Inorg. Biochem.* **2001**, *83*, 247−253.
(4) Nojiri, M.; Yohda, M.; Odaka, M.; Matsushita, Y.; Tsujimura, M.; Yoshida, T.; Dohmae, N.; Takio, K.; Endo, I. *J. Biochem.* (*Tokyo*) **1999**, *125*, 696−704.
(5) Murakami, T.; Nojiri, M.; Nakayama, H.; Odaka, M.; Yohda, M.; Dohmae, N.; Takio, K.; Nagamune, T.; Endo, I. *Protein Sci.* **2000**, *9*, 1024−1030.
(6) Shearer, J.; Kung, I. Y.; Lovell, S.; Kaminsky, W.; Kovacs, J. A. *J. Am. Chem. Soc.* **2001**, *123*, 463−468.
(7) Mascharak, P. K. *Coord. Chem. Rev.* **2002**, *225*, 201−214.
(8) Greene, S. N.; Richards, N. G. J. *Inorg. Chem.* **2004**, *43*, 7030−7041.
(9) Kovacs, J. A. *Chem. Rev.* **2004**, *104*, 825−848.

10.1021/ic070244l CCC: $37.00
Published on Web 05/15/2007

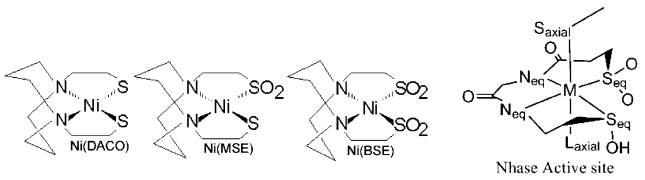

Figure 1. Schematic diagram of the model complexes used in this study. From left: Ni(DACO), Ni(MSE), Ni(BSE), and the active site of Nhase.

residues leads to inactivation of the enzyme, and they are proposed to be the source of protons during the reaction.[11,12] These studies have been complemented by spectroscopic and computational results that have focused on the electronic structure of the transition-metal active site.[8,13,14] Through such studies, a general consensus has been reached that these oxidized thiolate ligands are weak donors, and, hence, they increase the Lewis acidity of these active sites.[7,15]

A large number of Ni^{II} complexes have been reported to have a diamino−dithiolato coordination sphere where the thiolate has been systematically oxidized to RSO^- and RSO_2^-.[16−20] The crystallographically characterized complexes show that the Ni−S bond lengths decrease from 2.17 to 2.13 Å upon oxidizing RS^- to RSO_2^-.[17] Square-planar Ni^{II} complexes generally form only σ bonds due to the low-spin d^8 configuration. Shortening of a M−S bond length upon oxidation of a RS^- to RSO_2^- (by 0.04 Å) has also been observed for six-coordinate low-spin Co^{III} complexes, which are of low-spin d^6 and also allow for only σ interactions with these ligands.[21] The shorter M−S bond length of an oxidized thiolate is an apparent contradiction to the general idea that the S-donor strength decreases upon oxidation. Thus, a quantitative experimental estimate of the change in M−S bond covalency upon oxidation is required to elucidate the nature of bonding from the oxidized thiolate donors.

Ligand K-edge X-ray absorption spectroscopy (XAS) is a direct probe of ligand−metal bond covalency.[22,23] The K-edge spectra of transition-metal complexes have an intense low-energy pre-edge feature that is assigned as a ligand 1s (L_{1s}) to metal 3d (M_{3d}) transition. The pre-edge transition energy has contributions mainly from the effective nuclear charge (Z_{eff}) of the metal, its ligand field, and the charge on the ligand. Whereas the first two determine the energy of the acceptor M_{3d} orbital, the latter governs the energy of the donor ligand 1s orbital. The intensity (I) of this transition is given by

$$I(L_{1s} \rightarrow M_{3d}) = \alpha^2 I(L_{1s} \rightarrow L_{np}) \qquad (1)$$

where α is the ligand coefficient in the acceptor orbital wavefunction and $I(L_{1s} \rightarrow L_{np})$ is the transition moment integral or the intensity of a purely ligand-based 1s → np transition, which depends primarily on the Z_{eff} of the ligand.[24,25] The pure 1s → 3p dipole moment integral for a thiolate ligand (RS^-) was initially estimated from the pre-edge intensity of plastocyanin and recently was slightly modified from an increased data set.[24,26] The pre-edge intensity thus provides a direct estimate of ligand−metal bond covalency (α^2). The K-edge XAS of a thiolate-based ligand has additional higher energy features that are assigned as $S_{1s} \rightarrow RS_{C-S\sigma^*}$ transitions, which are a direct probe of the Z_{eff} on the ligand and thus show strong correlation to the oxidation state of the ligand.[23,27] These features have been used to identify the oxidation states of the oxidized thiolates of the active form of Fe-type Nhase in solution.[13]

This technique has recently been used to understand the effect of ligand oxidation on a low-spin Fe^{III} system where one of the two thiolate ligands of the parent complex is oxidized to S−O.[28] Upon oxidation, the Fe−S distances of the oxidized thiolate elongate and that of the remaining unoxidized thiolate decreases relative to the parent Fe−S thiolate distances. The changes observed in the S K-edge spectra reflect a large decrease in π donation of an oxidized thiolate relative to a thiolate. However, the effect of thiolate oxidation on the σ donation could not be quantified, as the S_{1s} orbital of these ligands is shifted to deeper energy, which in turn raises the pre-edge $S_{1s} \rightarrow Fe_{3d}$ transition energy such that it overlaps the rising-edge features from the unoxidized thiolate.[28]

In this study, we use sulfur K-edge XAS on a series of Ni^{II} complexes based on the *N*,*N*′-bis(2-mercaptoethyl)-1,5-diazacyclootanato (DACO) ligand system (Figure 1). The thiolates have been systematically oxidized to RSO_2^-, which provides an opportunity to experimentally probe the effect of thiolate oxidation on Ni−S σ-bond covalency. Our results indicate that the Ni−S bond of an oxidized thiolate is as

(10) Nagashima, S.; Nakasako, M.; Dohmae, N.; Tsujimura, M.; Takio, K.; Odaka, M.; Yohda, M.; Kamiya, N.; Endo, I. *Nat. Struct. Biol.* **1998**, *5*, 347−351.
(11) Miyanaga, A.; Fushinobu, S.; Ito, K.; Shoun, H.; Wakagi, T. *Eur. J. Biochem.* **2004**, *271*, 429−438.
(12) Piersma, S. R.; Nojiri, M.; Tsujimura, M.; Noguchi, T.; Odaka, M.; Yohda, M.; Inoue, Y.; Endo, I. *J. Inorg. Biochem.* **2000**, *80*, 283−288.
(13) Dey, A.; Chow, M.; Taniguchi, K.; Lugo-Mas, P.; Davin, S.; Maeda, M.; Kovacs, J. A.; Odaka, M.; Hodgson, K. O.; Hedman, B.; Solomon, E. I. *J. Am. Chem. Soc.* **2006**, *128*, 533−541.
(14) Boone, A. J.; Chang, C. H.; Greene, S. N.; Herz, T.; Richards, N. G. J. *Coord. Chem. Rev.* **2003**, *238*, 291−314.
(15) Harrop, T. C.; Mascharak, P. K. *Acc. Chem. Res.* **2004**, *37*, 253−260.
(16) Darensbourg, M. Y.; Font, I.; Mills, D. K.; Pala, M.; Reibenspies, J. H. *Inorg. Chem.* **1992**, *31*, 4965−4971.
(17) Farmer, P. J.; Reibenspies, J. H.; Lindahl, P. A.; Darensbourg, M. Y. *J. Am. Chem. Soc.* **1993**, *115*, 4665−4674.
(18) Bellefeuille, J. A.; Grapperhaus, C. A.; Buonomo, R. M.; Reibenspies, J. H.; Darensbourg, M. Y. *Organometallics* **1998**, *17*, 4813−4821.
(19) Chohan, B. S.; Maroney, M. J. *Inorg. Chem.* **2006**, *45*, 1906−1908.
(20) Chohan, B. S.; Shoner, S. C.; Kovacs, J. A.; Maroney, M. J. *Inorg. Chem.* **2004**, *43*, 7726−7734.
(21) Tyler, L. A.; Noveron, J. C.; Olmstead, M. M.; Mascharak, P. K. *Inorg. Chem.* **2000**, *39*, 357−362.
(22) Glaser, T.; Hedman, B.; Hodgson, K. O.; Solomon, E. I. *Acc. Chem. Res.* **2000**, *33*, 859−868.
(23) Solomon, E. I.; Hedman, B.; Hodgson, K. O.; Dey, A.; Szilagyi, R. K. *Coord. Chem. Rev.* **2005**, *249*, 97−129.
(24) Shadle, S. E.; Hedman, B.; Hodgson, K. O.; Solomon, E. I. *Inorg. Chem.* **1994**, *33*, 4235−4244.
(25) Neese, F.; Hedman, B.; Hodgson, K. O.; Solomon, E. I. *Inorg. Chem.* **1999**, *38*, 4854−4860.
(26) Shadle, S. E.; Penner-Hahn, J. E.; Schugar, H. J.; Hedman, B.; Hodgson, K. O.; Solomon, E. I. *J. Am. Chem. Soc.* **1993**, *115*, 767−776.
(27) Hedman, B.; Frank, P.; Gheller, S. F.; Roe, A. L.; Newton, W. E.; Hodgson, K. O. *J. Am. Chem. Soc.* **1988**, *110*, 3798−3805.
(28) Lugo-Mas, P.; Dey, A.; Xu, L.; Davin, S. D.; Benedict, J.; Kaminsky, W.; Hodgson, K. O.; Hedman, B.; Solomon, E. I.; Kovacs, J. A. *J. Am. Chem. Soc.* **2006**, *128*, 11211−11221.

Table 1. S K-Edge XAS Results

	RS^-				RSO_2^-			
	Ni_{3d} energy (eV)	intensity	covalency ($\%S_{3p}$/hole)	C−S σ^* energy (eV)	Ni_{3d} energy (eV)	intensity	covalency ($\%S_{3p}$/hole)	C−S σ^*+ S−O σ^* energy (eV)
Ni(DACO)	2470.8	1.25 ± 0.01	46 ± 2	2473.0				
Ni(MSE)	2470.7	0.68 ± 0.01	25 ± 2	2473.1	2476.1			2478.2
Ni(BSE)					2476.1	1.09 ± 0.01	18 ± 5	2478.2

covalent as that of an unoxidized thiolate. DFT calculations are used to develop a bonding description and to understand the covalency of the oxidized thiolate−sulfur−nickel bonds. These complexes model the mixed ligand environment present in the first coordination sphere of Nhase (Figure 1, right). We then used DFT calculations to explore the role of thiolate oxidations on the electronic structure and substrate binding affinity of Fe- and Co-type Nhases.

Experimental Details

Materials and Methods. The complexes Ni^{II} [*N*,*N*′-bis(2-mercaptoethyl)-1,5-diazacyclooctanato] (Ni(DACO)), Ni^{II} [*N*,*N*′-2-mercaptoethyl-2-sulfinatoethyl-1,5-diazacyclootanato] (Ni(MSE)), and Ni^{II} [*N*,*N*′-bis(2-sulfinatoethyl)-1,5-diazacyclooctanato] (Ni(BSE)) were synthesized according to the literature.[17,29] For XAS experiments, the samples were ground into a fine powder and dispersed as thinly as possible on sulfur-free Mylar tape. This procedure has been verified to minimize self-absorption effects.[27] The sample was then mounted across the window of an aluminum plate.

Data Collection. XAS data were measured at the Stanford Synchrotron Radiation Laboratory using the 54-pole wiggler beam line 6-2. Details of the experimental configuration for low-energy studies have been described previously. The energy calibration, data reduction, and error analysis follow the methods described in ref 24.

Fitting Procedures. The pre-edge features were fit by pseudo-Voigt line shapes (sums of Lorentzian and Gaussian functions) using *EDG_FIT*.[30] This line shape is appropriate, as the experimental features are expected to be a convolution of a Lorentzian transition envelope and a Gaussian line shape imposed by the beam line optics.[31,32] A fixed 1:1 ratio of Lorentzian-to-Gaussian contribution successfully reproduced the pre-edge features. The rising edges were also fit with pseudo-Voigt line shapes. Fitting requirements included reproducing the data and its second derivative, using the minimum number of peaks. In this case, we find that one peak was sufficient. The intensity of a pre-edge feature (peak area) is obtained from the product of peak height and full width at half-maxima of the pseudo-Voigt peaks, which were needed to successfully fit the feature in a given fit. The reported intensity values for the model complexes are an average of all the accepted pre-edge fits, typically 5−6 (which differed from each other by less than 3%). The fitted intensities were converted to $\%S_{3p}$ character using the pre-edge feature of plastocyanin as a reference (where 1.01 units of intensity, obtained using *EDG_FIT*, corresponded to 38% S_{3p} character).

DFT Calculations. All calculations were performed on dual-CPU Pentium Xeon 2.8 GHz work stations. Geometry optimizations for the Ni complexes were performed using the *Amsterdam Density Functional* (ADF) program, version 2004.01, and developed by Baerends et al.[33] A triple-ζ Slater-type orbital basis set (ADF basis set TZP) with a single polarization function at the local density approximation of Vosko et al.,[34] with the nonlocal gradient corrections of Becke[35] and Perdew,[36] was employed. For the Co and Fe Nhase active sites, the geometries were optimized in *Gaussian 03*[37] using the BP86[38] functional and a mixed basis set (6-311g* on Fe, Co, S, and N and 6-31g* on O, C, and H). All single point calculations were performed using the BP86 functional and a 6-311+g* basis set in *Gaussian 03*. The molecular orbitals were plotted using *Molden* version 4.1, and the Mulliken[39] population analyses were performed using the *PyMOlyze* program.[40]

Results and Analysis

1.1. Ni−S Bond Covalency: XAS. The S K-edge XAS of Ni(DACO) is shown in Figure 2 (black). The spectrum has a sharp feature at 2470.8 eV (Table 1), which is assigned to the $RS_{1s} \rightarrow Ni_{3d}$ *pre-edge* transition. The intensity of the pre-edge transition is directly proportional to the S_{3p} mixing in the acceptor Ni_{3d} LUMOs of these square-planar Ni^{II} complexes, i.e., Ni−S bond covalency. The pre-edge intensity of 1.25 units is obtained from fits to the experimental data. This intensity translates to 46% S_{3p} character in the acceptor Ni_{3d} orbital (Table 1), using thiolate as a reference. Note that this is a sum total contribution from two thiolates, i.e., the contribution from individual thiolates to the Ni_{3d} LUMO is 23%. There is another transition (*rising edge*) at 2473.0 eV (Table 1), which is assigned to the $RS_{1s} \rightarrow RS_{C-S\sigma^*}$ transition, and it is indicative of the oxidation state of the S atom.

The S K-edge XAS of Ni(MSE) (thiolate donor oxidized to RSO_2^-, red, Figure 2) has the pre-edge and the rising-edge transitions of the unoxidized thiolate ligand at 2470.7 and 2473.1 eV, respectively (Table 1), which are at the same energy and approximately half as intense as those in Ni-(DACO). This reflects the fact that Ni(MSE) has one RS^-

(29) Farmer, P. J.; Solouki, T.; Mills, D. K.; Soma, T.; Russell, D. H.; Reibenspies, J. H.; Darensbourg, M. Y. *J. Am. Chem. Soc.* **1992**, *114*, 4601−4605.
(30) George, G. N. *EXAFSPAK & EDG_FIT*; Stanford Synchrotron Radiation Laboratory, Stanford Linear Accelerator Center, Stanford University: Stanford, CA, 2000.
(31) Agarwal, B. *X-ray Spectroscopy*; Springer-Verlag: Berlin, 1979; pp 276 ff.
(32) Tyson, T. A.; Roe, A. L.; Frank, P.; Hodgson, K. O.; Hedman, B. *Physical Review B* **1989**, *39*, 6305−6315.
(33) Baerends, E. J.; Ellis, D. E.; Ros, P. *Chem. Phys.* **1973**, *2*, 41−51.
(34) Vosko, S. H.; Wilk, L.; Nusair, M. *Can. J. Phys.* **1980**, *58*, 1200−11.
(35) Becke, A. D. *J. Chem. Phys.* **1993**, *98*, 5648−5652.
(36) Perdew, J. P. *Physical Review B: Condensed Matter Mater. Phys.* **1986**, *33*, 8822−8824.
(37) Frisch, M. et. al. *Gaussian 03*, revision C.02; Gaussian, Inc.: Wallingford, CT, 2004. Full reference information is given in the Supporting Information.
(38) Becke, A. D. *Phys. Rev. A* **1988**, *38*, 3098−3100.
(39) Mulliken, R. S. *J. Chem. Phys.* **1955**, *23*, 1833−1840.
(40) Tenderholt, A. L. *PyMOlyze*, version 1.1. http://pymolyze.sourceforge.net.

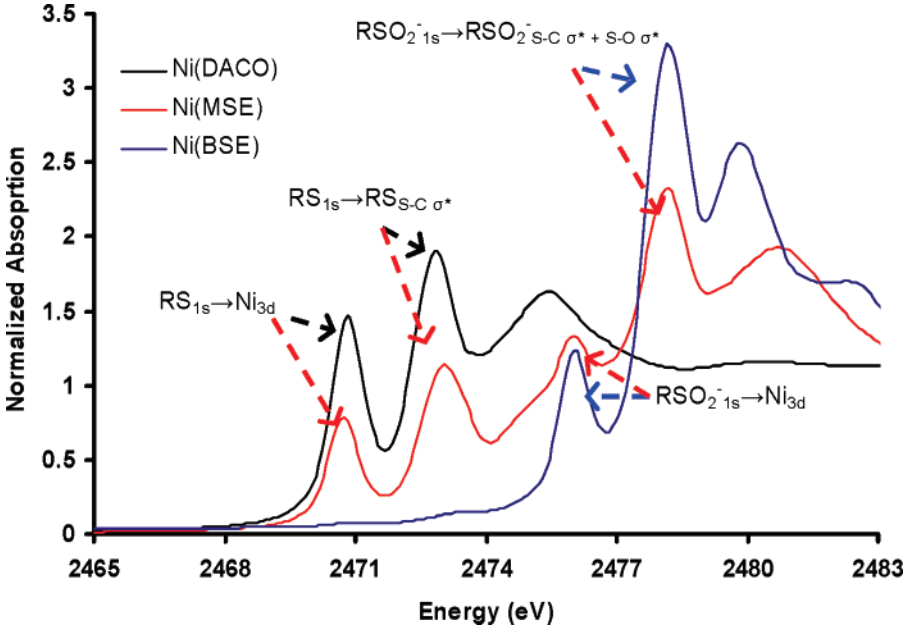

Figure 2. S K-edge XAS data of Ni(DACO) (black), Ni(MSE) (red), and Ni(BSE) (blue). The relevant pre-edge and rising-edge transitions are labeled. For assignments of these features, see ref 23.

donor relative to two donors in Ni(DACO). The $RSO_2^-{}_{1s} \rightarrow Ni_{3d}$ and the $RSO_2^-{}_{1s} \rightarrow RSO_2^-{}_{C-S\sigma^*+S-O\sigma^*}$ transitions are observed at 2476.1 and 2478.2 eV (Table 1), respectively. Due to the overlap of the pre-edge feature of RSO_2^- with the rising edge of the RS^-, it is not possible to obtain unambiguous estimates of the pre-edge intensity for the RSO_2^- ligand of this complex. However, these transitions are clearly visible in the S K-edge XAS spectrum of the Ni(BSE) complex (blue, Figure 2), where both thiolate ligands are oxidized to RSO_2^-. Both the pre-edge and the rising-edge features are shifted up by ~5 eV relative to the corresponding RS^- transitions, reflecting the stabilization of the S_{1s} orbitals in the RSO_2^- ligand upon oxidation. The intensity of this pre-edge transition is obtained from fits to the data and is given as 1.37 units. Note that this intensity cannot be directly converted to $\%S_{3p}$ mixing in the acceptor Ni_{3d} orbital, as I (transition moment integral) in eq 1 increases with Z_{eff}, and there is no well-defined reference allowing for the estimation of the transition dipole integral for an oxidized RSO_2^- donor. However, I was found to increase linearly with an increase in the relative 1s orbital energies of the different sulfur-based donors.[25,41,42] Note that the relative S_{1s} orbital energies cannot be obtained from the rising edges of the free ligands, as the acceptor orbitals (e.g., C−S σ^* in thiolate vs C−S σ^* and S−O σ^* in RSO_2^-, etc.) of these ligands are at different energies.

The relative 1s orbital energies for the RS^- and the RSO_2^- ligands can be accurately obtained from their relative pre-edge energies in the S K-edge XAS of Ni(MSE). This is because these involve transitions from the two different S-based donors to the same Ni_{3d} acceptor orbital. Thus, the relative pre-edge energies of $RS^-$and RSO_2^- at 2470.7 and 2476.1 eV, respectively, imply a 5.4 eV difference in the 1s orbital energy of these ligands. With the use of this 5.4 eV shift and the linear relation between the 1s orbital energy and dipole integral ($\langle_{1s}|\mathbf{r}|S_{3p}\rangle$),[41,42] its value for RSO_2^- is estimated as 18.2 (the value for thiolate is 8.05).[41,43] The total intensity under the pre-edge of Ni(BSE) is 1.09 units, which corresponds to 18% S_{3p} character (Table 1) in the acceptor Ni_{3d} orbital in Ni(BSE). This is an apparent decrease from the 46% of Ni(DACO), even though the Ni−S bond length decreases upon oxidation. *Note that this is the first time that a direct experimental estimate of the covalency of a RSO_2^- ligand has been obtained.*

1.2. Ni−S Bond Covalency: DFT Calculations. Geometry-optimized DFT calculations were used to obtain a description of the ground-state electronic structure of these complexes to gain insight into the changes in bonding that occur upon S oxidation. The calculated Ni−S bond lengths are in good agreement with the reported crystal structures of these complexes, whereas the Ni−N bond lengths are ~0.06 Å longer (Table 2). Note that the optimized Ni−S bonds in Ni(BSE) (2.13 Å) are 0.04 Å shorter than the Ni−S bonds in Ni(DACO) (2.17 Å), reproducing the trend observed in the crystal structures.[17] The calculated MO diagrams show that Ni(DACO), Ni(MSE), and Ni(BSE) are d^8 square-planar diamagnetic species (consistent with experiment) with an unoccupied Ni $3d_{x^2-y^2}$ LUMO. This orbital has strong σ-antibonding interactions with S_{3p} and N_{2p} orbitals in all three complexes. The calculated S_{3p} character of the unoxi-

(41) Sarangi, R.; George DeBeer, S.; Rudd, D. J.; Szilagyi, R. K.; Ribas, X.; Rovira, C.; Almeida, M.; Hodgson, K. O.; Hedman, B.; Solomon, E. I. *J. Am. Chem. Soc.* **2007**, *129*.

(42) Szilagyi, R. K.; Lim, B. S.; Glaser, T.; Holm, R. H.; Hedman, B.; Hodgson, K. O.; Solomon, E. I. *J. Am. Chem. Soc.* **2003**, *125*, 9158−9169.

(43) Note that the intensity of the rising edge of a RSO_2^- ion is 4−5 times that of a thiolate ion. This increase partially reflects the fact that there is more $\%S_{3p}$ in the acceptor orbitals in RSO_2^- (calculated, 130%) due to the additional S−O σ^* orbitals relative to those in a thiolate ligand (calculated, 60%) along with the 2.25-fold increase in the transition moment integral.

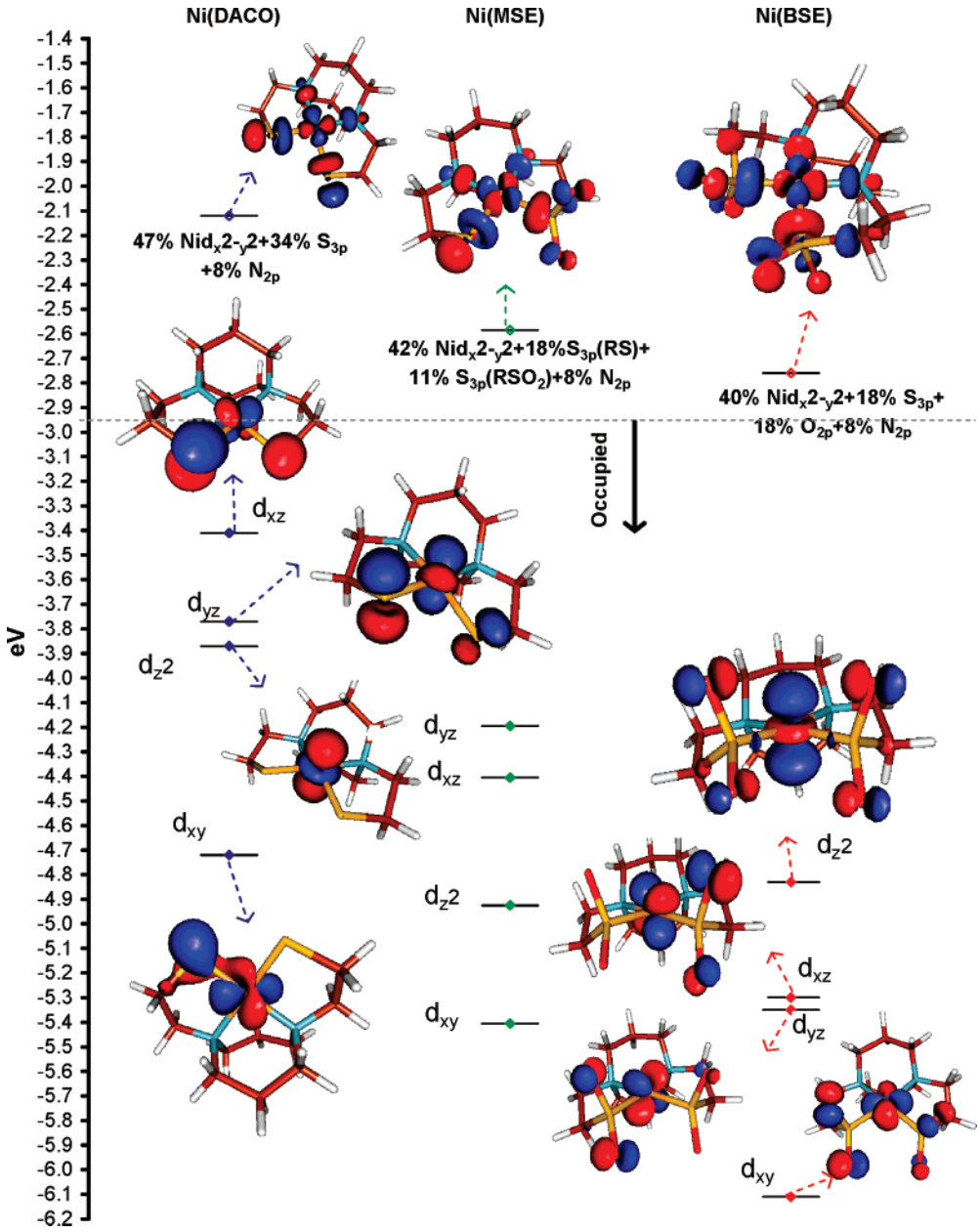

Figure 3. MO diagram of the complexes Ni(DACO), Ni(MSE), and Ni(BSE). The relevant Ni_{3d} contours are shown (occupied orbitals are indicated by filled diamonds). The contours of Ni(MSE) are similar to those of Ni(BSE), and hence, they are not shown to avoid crowding. The Ni_{3d}, S_{3p}, O_{2p}, and N_{2p} coefficients are indicated in the text. Orbitals above the dashed lines are unoccupied.

Table 2. DFT-Optimized Geometric Parameters (Crystallographic Distances in Parentheses)

	Ni−S (Å)	Ni−SO_2 (Å)	Ni−N (Å)	C−S (Å)	S−O (Å)
Ni(DACO)	2.17 (2.16)		2.04 (1.98)	1.84 (1.81)	
Ni(MSE)	2.18 (2.13)	2.15 (2.11)	2.06 (1.99)	1.84 (1.85) 1.86 (1.84)	1.49 (1.46)
Ni(BSE)		2.13 (2.13)	2.04 (2.00)	1.87 (1.83)	1.49 (1.45)

dized thiolate in the Ni_{3d} hole is 34% (two thiolates) and 18% (one thiolate) in Ni(DACO) and Ni(MSE), respectively. The calculated total S_{3p} character for the oxidized thiolates is 18% (summed over α and β holes) in Ni(BSE). These calculated values are in reasonable agreement with the experimental data obtained on Ni(DACO) (46%), Ni(MSE) (25%, only thiolate), and Ni(BSE) (18%) (Table 1).[44]

The total Ni_{3d} character percentages in Ni(DACO) and Ni(BSE) are 47 and 40% in the acceptor $3d_{x^2-y^2}$ LUMOs, respectively. This implies that the Ni(BSE) system is more covalent than the Ni(DACO) system, which is not consistent with the idea that an oxidized RSO_2^- ligand is a poorer donor than a RS^- ligand. The calculated $\%S_{3p}$ character in the LUMO decreases from 36% in Ni(DACO) to 18% in Ni(BSE), consistent with the experimental data (Table 1). However, the decrease in the calculated Ni_{3d} and S_{3p} character from Ni(DACO) to Ni(BSE) is associated with an increase in the O_{2p} character in the RSO_2^- fragment in the LUMO (Figure 3). Thus, the total RSO_2^- ligand contribution to the $3d_{x^2-y^2}$ LUMO is 42% in Ni(BSE), which explains its higher covalency relative to that of Ni(DACO) (36% RS^- character

(44) Note that the experimentally obtained Ni−S covalency is higher than the calculated value. This is commonly observed at this level of theory. This can also have some contribution from a 0.01 Å longer Ni−S bond in the optimized structures.

Scheme 1. Schematic MO Diagram of an RSO_2^- Fragment (right) Correlated to Parent RS^- MOs (left)[a]

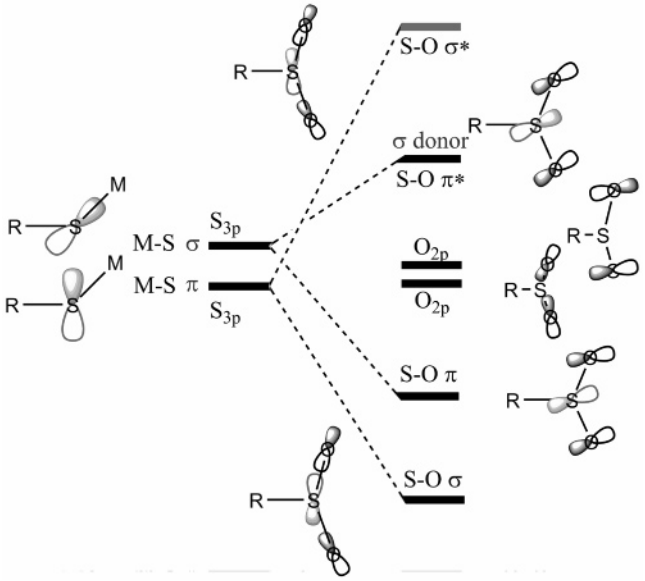

[a] The nature of the MOs and the type of donor interaction of an orbital with a metal center are indicated. Only four O_{2p} orbitals (two each on the SO_2^- oxygen) that interact with the S_{3p} orbital are shown in this scheme. The third set of the O_{2p} orbital is nonbonding. The MOs indicated by black lines are occupied, and the one indicated by a gray line is unoccupied.

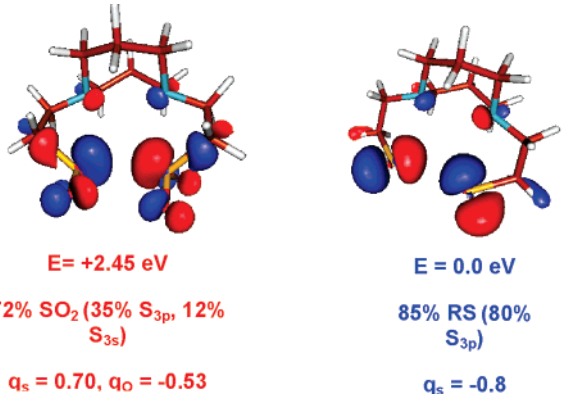

Figure 4. Donor valence orbitals of the RSO_2^- and RS^- ligands including the effect of the charge of a central Ni atom (modeled as a point charge).

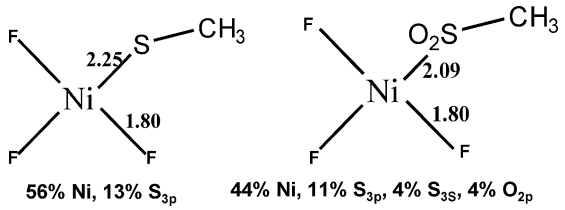

Figure 5. Geometry-optimized parameters of NiF_3X (X = RS^- in left and RSO_2^- in right) systems.

in the LUMO). The mixing of the O_{2p} character into the Ni_{3d} LUMO indicates that the donor orbitals in the BSE ligand are delocalized over the RSO_2^- fragment.

DFT calculations were performed on free ligands to analyze the mixing of O_{2p} in the LUMO of Ni(BSE). These calculations show (Scheme 1) that the RSO_2^- ligand has valence orbitals that are delocalized over the SO_2^- unit available for bonding. The thiolate S valence orbital, which will π-donate to a metal, interacts with one O_{2p} orbital on each of the two O atoms in RSO_2^- to form a S−O σ-bonding, an O_{2p}-based nonbonding, and a S−O σ*-antibonding orbital. The orbital of the thiolate, which would σ-donate to the metal, likewise interacts with two O_{2p} orbitals (one from each oxygen atom of RSO_2^-) to form a S−O π-bonding, an O_{2p}-based nonbonding, and a S−O π*-antibonding orbital. Out of these six RSO_2^- MOs, the S−O σ- and π-bonding orbitals are occupied and stabilized in energy such that they cannot efficiently interact with the metal. The S−O σ* orbital is unoccupied and thus does not donate to the metal. Note that we are ignoring the possibility that O_{2p}-based nonbonding orbitals can serve as donor orbitals, as they are not directly coordinated to the metal. The only possible donor interaction is with the S−O π*-antibonding orbital, which is occupied, at a higher energy relative to that of a thiolate (owing to its π* nature), and is oriented along the S−M bond and thus can form a covalent σ bond with the metal center.

The covalency of a metal−ligand bond is directly proportional to the overlap (H_{ML}) and inversely proportional to the energy separation between the metal acceptor and the ligand donor orbital (Δ) before bonding. The H_{ML} term favors the RS^- ligand due to there being 80% S_{3p} character in the RS^- donor orbital relative to 35% S_{3p} character in RSO_2^- (S atom coordinated in both cases). However, the relative energies of these donor orbitals are affected by the oxidation state of the S atom, the π-antibonding nature of the RSO_2^- donor orbital, and by Coulombic interaction with the positively charged Ni^{II} center. The formal oxidation states of the S's are +2 and −2, and the charges on the S's in the calculations are +0.7 and −0.8 for RSO_2^- and RS^-, respectively. The higher oxidation state of S in RSO_2^- will tend to stabilize this donor orbital whereas the higher positive charge on the S atom in RSO_2^- will destabilize it relative to the donor orbitals of a RS^- ligand upon interaction with the positively charged Ni. Additionally, the π-antibonding nature of the RSO_2^- donor orbital raises its energy relative to that of a S_{3p}-based RS^- donor orbital. The resultant donor-orbital descriptions (including the effect of Ni charge) and their relative energies are shown in Figure 4. The delocalized RSO_2^- donor orbital (Figure 4, left), with only 35% S_{3p}, is 2.5 eV higher in energy than the mainly S_{3p}-based RS^- donor orbital (with 80% S_{3p}). Thus, although the overlap will be less, due to the reduced S character, the favorable energies of the donor orbital of RSO_2^- result in a very covalent interaction with the metal, as observed in the experimental data and the calculations. Also, the RSO_2^- ligand has a shorter Ni−S distance (2.13 Å in Ni(BSE) relative to that of 2.17 Å in Ni(DACO)), which reflects its observed net higher covalency.

2. Ni−S Bond Length. The crystallographically obtained Ni−S bond length in Ni(BSE) is 2.13 Å, which is 0.04 Å shorter than the Ni−S bond distances in the Ni(DACO) dithiolate. Several possible factors could contribute to the shortening of the Ni−S bonds with an oxidized RSO_2^- donor: (1) Constraints of the ligand framework, (2) increased ionic interaction of the Ni^{II} with the oxygens in the RSO_2^- ligand, and (3) decreased electron repulsion between the Ni_{3d} and the nonbonding π-donor S_{3p} orbitals of a thiolate upon

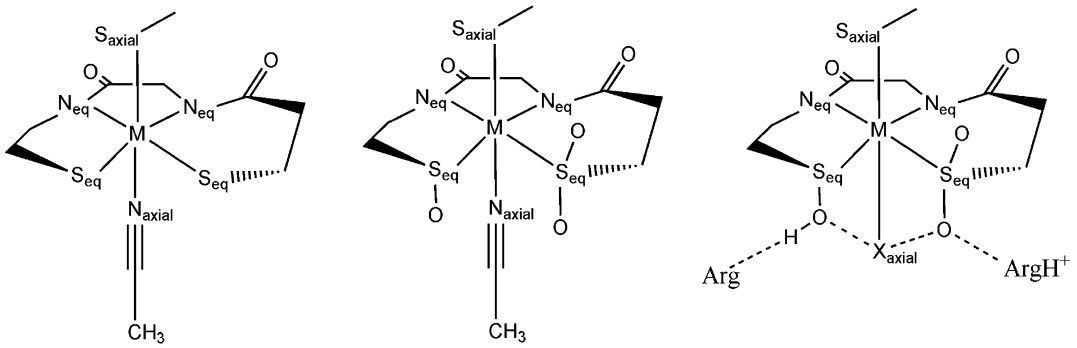

Figure 6. Models of CH_3CN-bound forms of the oxidized (middle) and unoxidized (left) forms and the H-bonding interaction in the modified active site (right) of Nhase.

oxidation.[18] To evaluate the effect of the macrocyclic ligand, geometry optimizations of simpler systems $[NiF_3X]^{2-}$ (where $X = RS^-$ or RSO_2^-) were performed. These calculations reproduce (Figure 5) the Ni−S bond shortening in RSO_2^- (2.09 Å) relative to that of RS^- (2.25 Å). Also, the calculated charge (NPA) on the S atom in the RSO_2^- is estimated to be +0.7 relative to that of −0.8 in RS^-, which disfavors the Ni−S bond shortening in the former due to its increased electrostatic repulsion. These results imply that the primary contribution to the Ni−S bond shortening in RSO_2^- may be the reduction of e−e repulsion between the filled Ni_{3d} (mainly *xz*, *yz*) and out-of-plane S_{3p} orbitals. This repulsion energy between the Ni^{2+} and the ligand fragments was calculated using the Pauli repulsion term in the Zeigler energy decomposition scheme available in the ADF package.[33,45] In Ni(BSE), a decrease in the Ni−S bond length from 2.17 Å (observed in the thiolates) to the optimized 2.13 Å leads to an increase in the filled−filled repulsion by 1.07 eV. The associated increase in bonding interactions compensates for this. Alternatively, in Ni(DACO) the same contraction of the Ni−S bond length leads to a 4.29 eV increase in the filled−filled repulsion, which is not compensated for by an increase in bonding. Thus, the oxidation of RS^- results in the stabilization of the out-of-plane nonbonding S_{3p} orbital due to the formation of a S−O σ bond, which reduces the interaction of this electron pair with the filled Ni_{3d} orbitals.[46] Though this filled−filled interaction does not affect the covalent contribution to the Ni−S bond energy, it manifests itself in the nature of the HOMO in these complexes. The HOMO in Ni(DACO) is the d_{xz} orbital, which has a very strong π-antibonding interaction with the out-of-plane S_{3p} donor orbitals. In Ni(BSE), this orbital is stabilized, as it lacks this π-antibonding interaction with the out-of-plane S_{3p} orbital, and the d_z2 orbital is the HOMO (Figure 3).

(45) te Velde, G.; Bickelhaupt, F. M.; van Gisbergen, S. J. A.; Fonseca Guerra, C.; Baerends, E. J.; Snijders, J. G.; Ziegler, T. *J. Comput. Chem.* **2001**, *22*, 931−967.

(46) A single point calculation of NiF_3RSO_2 with the Ni−S bond length fixed at 2.25 Å (i.e., the bond length of a Ni−SR bond) shows that even at a longer Ni−S distance, this system is very covalent (%Ni3d = 62%), which provides a driving force for the bond shortening once the e−e repulsion along the Ni−S bond is reduced upon oxidation.

Discussion

The experimental and computational results on the Ni^{II} series in Figure 1 provide evidence that oxidized RSO_2^- ligands are in fact strong σ donors. This derives from the higher energies of the oxidized S−O π^* orbital, which acts as the σ donor to the metal center. This higher energy is due to the π^* nature of the orbital and the positive charge on the S, which is destabilized upon electrostatic interaction with the Ni. However, in contrast to RS^-, RSO_2^- ligands are not involved in π donation, as this S_{3p} orbital is stabilized and localized due to the formation of strong S−O σ bonds.

The S K-edge XAS data in the mixed ligand complex Ni(MSE) show that the Ni−S covalency of the unoxidized thiolate remains unchanged upon oxidation of the adjacent thiolate donor. This spectator effect supports the idea that the oxidized RSO_2^- is still a strong σ donor and needs no compensation in a σ-bonding-only system like square-planar Ni^{II}. That is, the oxidation of one thiolate to RSO_2^- does not induce additional electron donation from the unmodified thiolate.

The lack of a compensatory effect in the nickel thiolate/sulfinate complex is in contrast to the results obtained on a low-spin Fe^{III} system where experimental data indicated that modification of a thiolate to RSO^- decreased its net charge donation to the Fe^{III}.[28] An unoxidized thiolate spectator ligand, in turn, became a much stronger donor, which compensated for the loss of charge donation from the oxidized thiolate. The different behavior in these two systems (low-spin Fe^{III} and Ni^{II}) arises from the difference in bonding interactions of these metals with the thiolate-based ligands. In low-spin Fe^{III}, both π- and σ-donor interactions are present and the t_2^5 configuration requires that the π-donor orbitals from the two thiolate ligands compete for the singly occupied d−π molecular orbital (SOMO) for bonding. Thus, oxidizing a thiolate eliminates its π-donor interaction, which reduces the total charge donation from this thiolate and enhances the π donation by the unoxidized thiolate. However, in the square-planar Ni^{II} system studied here, only σ interactions are possible. As the oxidized thiolate ligand RSO_2^- is still a good σ-donor ligand (using its S−O π^* orbital), there is no decrease in charge donation upon oxidation of the thiolate; hence, no increase in charge donation from the unoxidized thiolate is observed. It is interesting to note that if we extend

Table 3. DFT-Optimized Distances (Å) of Oxidized and Unoxidized Fe- and Co-Type Nhase

model	$M-S_{axial}$	$M-S_{eq}$	$M-N_{eq}$	$M-N_{axial}$
Fe unoxidized	2.22	2.30, 2.31	1.96, 2.00	2.53
Fe oxidized	2.25	2.24, 2.25	1.96, 1.97	1.99
Co unoxidized	2.35	2.35, 2.36	1.93, 1.97	1.83
Co oxidized	2.33	2.33, 2.25	1.94, 2.00	1.81

these results computationally to the hypothetical Ni^{III} complexes, a decrease in total charge donation from RSO_2^- relative to RS^- is now observed. Although in Ni^{III}(DACO) the d$-\pi$ SOMO of Ni^{III} has 16% S_{3p} on each thiolate, the $\%S_{3p}$ of the oxidized thiolate in the d$-\pi$ SOMO of Ni^{III}-(MSE) decreases to 0% and the $\%S_{3p}$ of the remaining unoxidized thiolate (Figure S1, Supporting Information) increases to 50% as it compensates for the loss of π donation from the other thiolate upon oxidation to RSO_2^-.

The lack of π donation by an oxidized thiolate ligand was proposed to result in an increased sixth-ligand-binding affinity in the oxidized active site of Fe^{III}-type Nhase.[23] Our results here suggest that the oxidized thiolates are as strong σ donors as the unoxidized thiolates. Thus, one may expect some differences in the role played by oxidized thiolates between the low-spin Fe^{III} (with both π and σ interactions in the t_2^5 configuration) and Co^{III} (with only σ interaction in the t_2^6 configuration) Nhases. DFT calculations were used to evaluate these possible differences. The optimized structures of the six-coordinate unoxidized (three RS^-, two amide donors, and CH_3CN, Figure 6, left) and oxidized (a RS^-, a RSO^-, a RSO_2^-, two amide donors, and CH_3CN, Figure 6, middle) active sites of Nhase were obtained. The Fe^{III} Nhase had optimized $Fe-N_{axial}$ CH_3CN distances of 2.53 and 1.99 Å for the unoxidized and the oxidized active site, respectively (Table 3, rows 1 and 2). These results parallel those obtained in ref 23 using H_2O as an axial ligand. In contrast, the calculations for the Co^{III} active site of Nhase show that the axial ligand is already strongly bound in the unoxidized active site and there is no significant change in the axial ligand-binding affinity for the oxidized active site (optimized $Co-N_{axial}$ distances are 1.83 and 1.81 Å, respectively (Table 3, rows 3 and 4)). The binding of the axial ligand in the low-spin Co^{III} (t_2^6) active site indicates its higher Lewis acidity due to a lack of d$-\pi$ donor bonding, which is present in the low-spin Fe^{III} (t_2^5) active site (as indicated by the shorter $Fe-S_{axial}$ distance relative to the $Co-S_{axial}$ distance in the unoxidized active site in Table 3). Upon oxidation of the equatorial thiolates, their π donation to the low-spin Fe d$-\pi$ orbital decreases and this increases its Lewis acidity and enhances binding of the axial CH_3CN ($Fe-N_{axial} = 1.99$ Å). No significant difference in the axial CH_3CN binding affinity of the σ-bonding Co active site is observed upon oxidation of the equatorial thiolates.

This suggests that although the oxidized cysteine ligands likely play a role in tuning the Lewis acidity of the Fe active site, this does not appear to be necessary in the Co active site. The post-translational modification of one of the cysteines to $S-O^-$ may play the role of a proton source for this hydrolytic reaction, as it is found to be protonated under physiological conditions.[13] The SO_2^- ligand may play a role in axial ligand binding by H bonding and proton shuttling between the axial ligand and nearby arginine residues (Figure 6, right), as suggested by mutational studies.[12]

Acknowledgment. This research was supported by NIH Grants 040392 (E.I.S.), RR-01209 (K.O.H.), NSF CHE 06-11695 (M.Y.D.). SSRL operations are supported by the Department of Energy, Office of Basic Energy Sciences. The SSRL Structural Molecular Biology Program is supported by the National Institutes of Health, National Center for Research Resources, Biomedical Technology Program, and by the Department of Energy, Office of Biological and Environmental Research.

Supporting Information Available: Optimized geometries of the Ni complexes and the Nhase active sites. This material is available free of charge via the Internet at http://pubs.acs.org.

IC070244L